


Article

Removal of Toxic Copper Ion from Aqueous Media by Adsorption on Fly Ash-Derived Zeolites: Kinetic and Equilibrium Studies

Gabriela Buema ¹, Luisa-Maria Trifas ² and Maria Harja ^{2,*} 

¹ National Institute of Research and Development for Technical Physics, 47 Mangeron Boulevard, 700050 Iasi, Romania; gbuema@phys-iasi.ro

² Faculty of Chemical Engineering and Environmental Protection, “Gheorghe Asachi” Technical University of Iasi, 73 Prof.dr.doc. Dimitrie Mangeron Street, 700050 Iasi, Romania; trifas.luisa@yahoo.com

* Correspondence: mharja@tuiasi.ro; Tel.: +40-747-909-645

Abstract: This study investigated the adsorption capacity of one material based on the treatment of fly ash with sodium hydroxide as a novel adsorbent for toxic Cu²⁺ ion removal from aqueous media. The adsorbent was obtained through direct activation of fly ash with 2M NaOH at 90 °C and 6 h of contact time. The adsorbent was characterized by recognized techniques for solid samples. The influence of adsorption parameters such as adsorbent dose, copper initial concentration and contact time was analyzed in order to establish the best adsorption conditions. The results revealed that the Langmuir model fitted with the copper adsorption data. The maximum copper adsorption capacity was 53.5 mg/g. The adsorption process followed the pseudo-second-order kinetic model. The results indicated that the mechanism of adsorption was chemisorption. The results also showed the copper ion removal efficiencies of the synthesized adsorbents. The proposed procedure is an innovative and economical method, which can be used for toxicity reduction by capitalizing on abundant solid waste and treatment wastewater.

Keywords: copper adsorption; fly ash; NaOH treatment; zeolite



Citation: Buema, G.; Trifas, L.-M.; Harja, M. Removal of Toxic Copper Ion from Aqueous Media by Adsorption on Fly Ash-Derived Zeolites: Kinetic and Equilibrium Studies. *Polymers* **2021**, *13*, 3468. <https://doi.org/10.3390/polym13203468>

Academic Editor: Tetyana Budnyak

Received: 20 September 2021

Accepted: 6 October 2021

Published: 9 October 2021

Publisher's Note: MDPI stays neutral with regard to jurisdictional claims in published maps and institutional affiliations.



Copyright: © 2021 by the authors. Licensee MDPI, Basel, Switzerland. This article is an open access article distributed under the terms and conditions of the Creative Commons Attribution (CC BY) license (<https://creativecommons.org/licenses/by/4.0/>).

1. Introduction

Copper ion is considered a toxic substance [1], whose health effects include stomachache, lung cancer and neurotoxicity. Copper and its compounds are widely used in many industries, such as: metal finishing, electroplating, plastics and etching [2]. A variety of traditional techniques for water treatment have been shown to be capable of removing copper from wastewater, including chemical precipitation, membrane filtration and ion exchange [3]. Adsorption can be explained as a separation process in which the components of a fluid phase are transferred to the surface of a solid material [4,5]. The adsorption process is the most used technique due to its efficiency and simplicity [6–8]. Several adsorbents have been tested in order to remove copper ion, such as activated carbon [8–10], clays [11], apatite [12], composite carbon-silica [13], magnetic materials [14–16], silica gel [17], hydroxyapatite [18], zeolites [19] and fly ash [5,20]. Over time, fly ash has been investigated by many researchers as an adsorbent for heavy metal removal [21,22]. The fly ash produced by coal combustion is a mixture of oxides with negative surface charge. The chemical composition of fly ash produced from different types of coal has been listed in the literature [22,23]. In accordance with ASTM C618, fly ash can be classified into two classes, depending on the sum of SiO₂, Al₂O₃ and Fe₂O₃ [24]. Generally, the amount of alkalis (combined sodium and potassium) and sulphates are higher in Class C than in Class F. Ash is one of the most complex materials that can be characterized. There are approximately 316 individual minerals and 188 mineral groups that have been identified in different ashes [25]. For most ashes, the major phases consist of mullite, quartz and hematite [26].

The mineralogical classification system divides ash into four types—pozzolanic (P), inert (I), active (A) and mixed (M)—based on the distinct behavior between (1) the vitreous phase, (2) quartz + mullite and (3) the sum of other mineral phases, such as Fe–Ca–Mg–K–Na–Ti–Mn oxyhydroxides, sulphates, carbonates and silicates.

Fly ash, as an adsorbent, is associated with some problems, such as a small surface area (which leads to low adsorption capacities) and low storage [20]. On the other hand, the production of fly ash is an environmental problem; there are on-going efforts to find a use for this waste [27].

Dinah et al. have shown that the ash can be treated with alkaline solutions [28]. Obtaining these types of materials represents one of the most important applications of fly ash [29].

One intensive application of fly ash is as an adsorbent for heavy metal removal from aqueous media [22]. In the actual scientific context, it is underlined that implementing a cheap and highly efficient adsorbent to treat water contaminated with copper ions is an interesting challenge. In their investigations, many researchers tried to make fly ash more usable by its surface modification, subsequently trying to make useful products from the industrial waste. Therefore, fly ash treated with NaOH has become a subject of interest in heavy metal removal [20,30–34].

The authors have studied heavy metal removal onto fly ash and modified ash, and through over 10 years of experience have demonstrated that at low concentrations of activators, the performances of the obtained materials are limited [35]. This study demonstrates that an excellent adsorption capacity can be obtained, and for cheaper conditions if the other factors are appropriate. This research provides insights into the interaction mechanisms of modified fly ash with copper ions, facilitating the application of this type of material as an adsorbent. Unmodified fly ash shows a low adsorption capacity for Cu^{2+} ions, of approximately 14 mg/g [14]. Therefore, the main idea of the present study is to investigate the removal of Cu^{2+} toxic pollutants using an adsorbent based on fly ash treated with NaOH. The adsorbent is characterized using SEM (scanning electron microscopy), EDX (energy dispersive X-ray), XRD (X-ray diffraction), FTIR (Fourier transform infrared spectroscopy), and BET (Brunauer–Emmett–Teller surface area) analyses. Copper ion adsorption is examined within the adsorbent dose, initial concentration and contact time from an aqueous media. The equilibrium adsorption data are analyzed using two adsorption isotherm models: Langmuir and Freundlich. Two kinetic models are applied: pseudo-first-kinetic and pseudo-second-order.

The data obtained in this study demonstrate that the low-cost and easy synthesis of this new material based on the treatment of raw fly ash with sodium hydroxide in combination with its properties represents a promising adsorbent for copper ion removal.

2. Materials and Methods

2.1. Materials

The starting material used for the synthesis of the adsorbent was fly ash collected from the thermoelectrical power plant Holoca (Iasi, Romania). All the reagents used in this study were purchased from Chemical Company (Iasi, Romania) and did not require further purification.

2.2. Preparation of Adsorbent

To fabricate the adsorbent, a solution of NaOH (2M) and fly ash was prepared in a mixture of 3:1 ratio and stirred for 6 h at 90 °C. Afterwards, the resulting adsorbent was separated from the solution and rinsed several times with distilled water until it achieved a neutral pH. Then, it was dried at 60 °C for 24 h and stored.

2.3. Material Characterization

The following instrumental studies were performed in order to characterize the prepared adsorbent: SEM, EDX, XRD, FTIR and BET. The SEM and EDAX analyses were de-

terminated with a Quanta 3D instrument AL99/D8229 (FEI Company, Hillsboro, OR, USA). X-ray powder diffraction was conducted using an X'Pert PRO MRD X-ray diffractometer (PANalytical, Almelo, The Netherlands). The experiment was recorded by monitoring the diffraction pattern appearing in the 2θ range from 10° to 90° . Infrared absorption spectra ($400\text{--}4000\text{ cm}^{-1}$) were analyzed with a Thermo Scientific Nicolet 6700 FT-IR spectrometer (Thermo Fisher Scientific, Waltham, MA, USA). BET surface area analysis was performed via Quantachrome instruments (Boynton Beach, FL, USA).

2.4. Batch Adsorption Experiments

Adsorption experiments were performed at room temperature, pH 5, at a shaking frequency of 300 rpm. Sample aliquots were collected after performing adsorption tests; the absorbance was measured at 390 nm wavelength using rubeanic acid [36]. Table 1 presents the adsorption experiments' conditions. A Buck Scientific spectrophotometer (Buck Scientific, East Norwalk, CT, USA) was used for copper ion determination.

Table 1. Adsorption experiment conditions.

Effect of Working Parameters	Adsorbent Dose	Initial Concentration	Contact Time
Effect of adsorbent dose	1 g/100 mL, 2 g/100 mL, 3 g/100 mL, 4 g/100 mL	300 mg/L	24 h
Effect of initial concentration	1 g/100 mL	100–700 mg/L	24 h
Effect of contact time	1 g/100 mL	300 mg/L	1–240 min

The adsorption capacity of the adsorbent, q (mg/g), was calculated based on Equation (1), and the adsorption efficiency was determined using Equation (2):

$$q = \frac{(C_i - C_e)V}{m} \quad (1)$$

$$\text{Adsorption efficiency, \%} = \frac{(C_i - C_e)}{C_i} \times 100 \quad (2)$$

where C_i (mg/L) represent the initial concentration of Cu^{2+} solution, C_e (mg/L) is the concentration of Cu^{2+} solution at equilibrium, V (L) is the volume of solution and m (g) is the quantity of the adsorbent used.

3. Results

3.1. Characterization of Adsorbent

SEM analysis was used in order to identify the surface morphology of the synthesized material, Figure 1a. A significant change in the material morphology was observed after treatment with NaOH at 90°C , as confirmed by the SEM images. This change may be attributed to the chemical method by which NaOH was diffused into the structure of the fly ash.

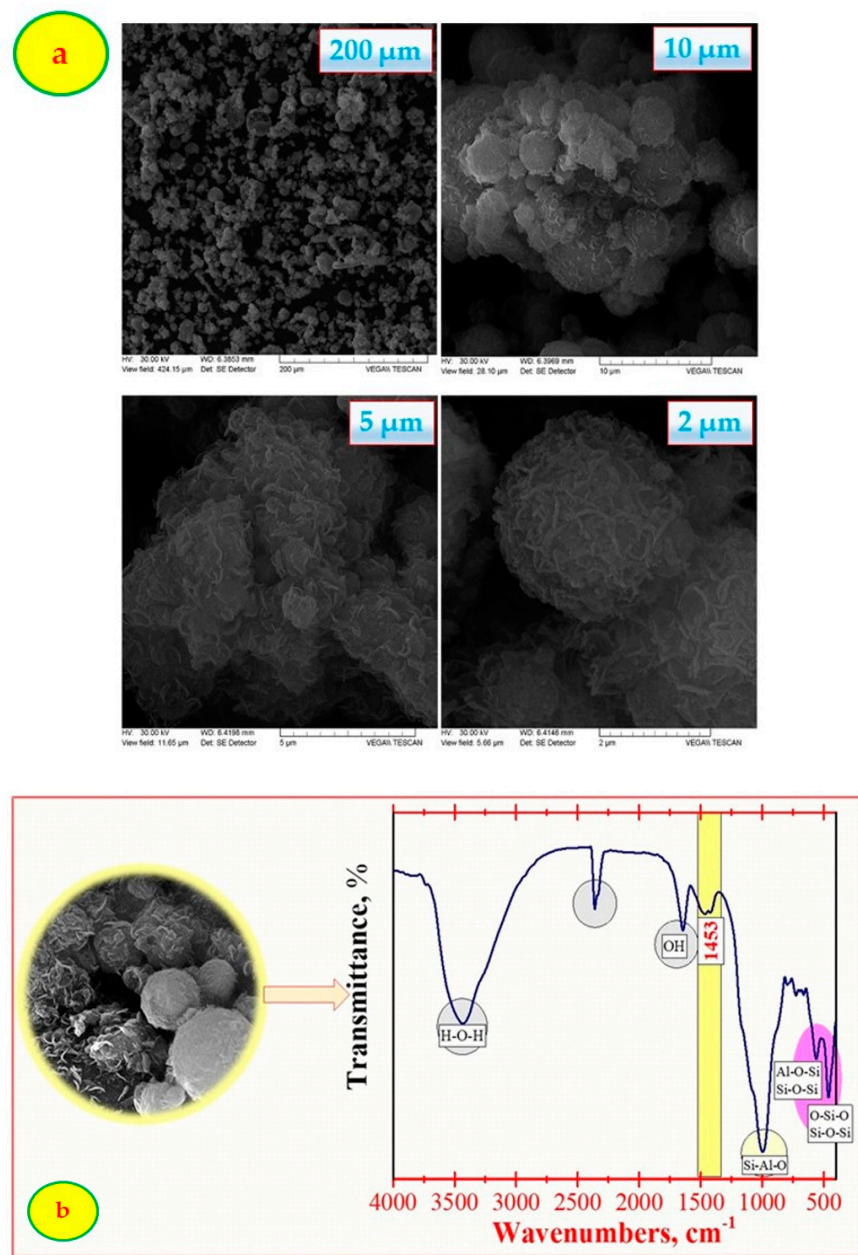


Figure 1. Cont.

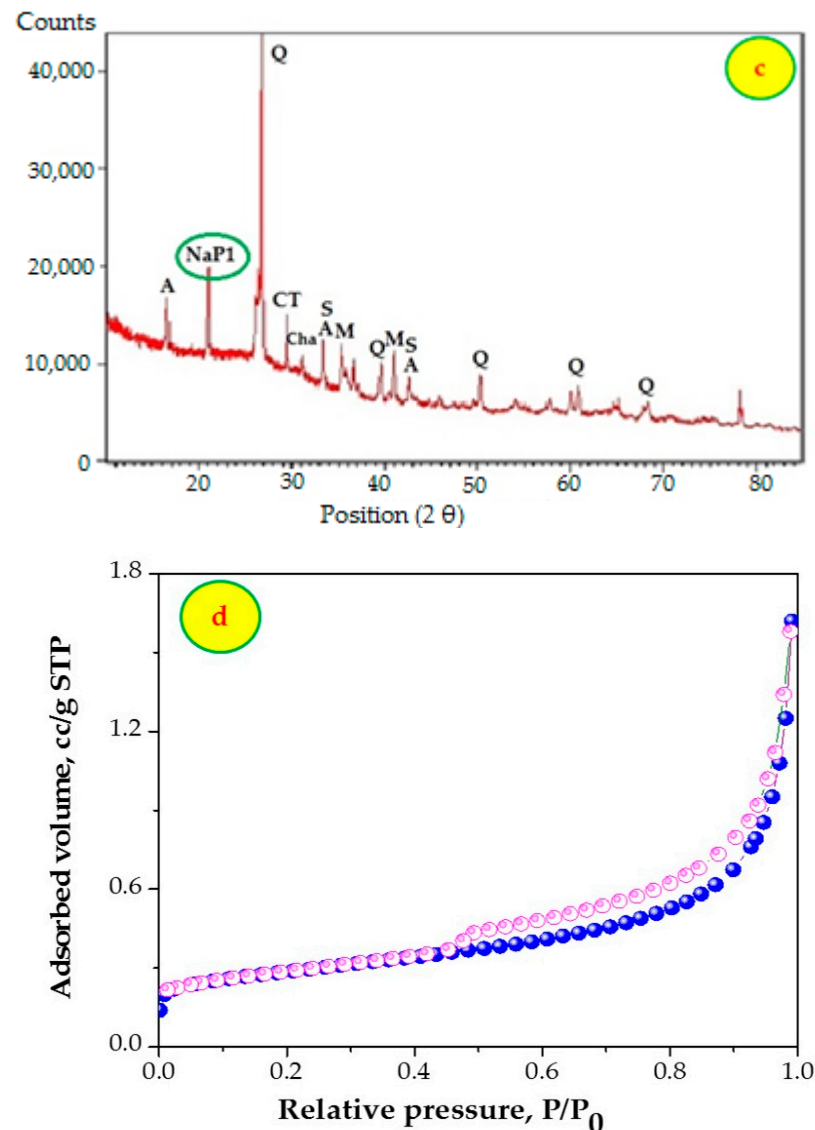


Figure 1. Characterization of the adsorbent: (a) SEM analysis; (b) FTIR analysis; (c) XRD analysis; (d) BET analysis.

The chemical composition of the material (Table 2), determined by EDX, indicated that the adsorbent contains Si, O, Al, Fe, Ca and Mg as well as small quantities of Ti, K and Na. The $\text{SiO}_2/\text{Al}_2\text{O}_3$ ratio was approximately 1.3, which is in the range of NaP-type zeolites [37].

Table 2. EDX analysis, % atomic.

O	Na	Mg	Al	Si	K	Ca	Ti	Fe
31.98	3.42	1.02	13.29	16.97	0.68	2.31	1.03	8.02

According to Figure 1b, the main functional groups were found at 3441 cm^{-1} , 2362 cm^{-1} , 1453 cm^{-1} , 1645 cm^{-1} , 1054 cm^{-1} , 558 cm^{-1} and 466 cm^{-1} . The peak at 2362 cm^{-1} can be assigned to the hydration water. The peak at 1453 cm^{-1} indicates that the sample included a GIS–NaP1 phase, a fact additionally demonstrated through the XRD analysis (Figure 1c). XRD analysis was interpreted according to the high-quality investigations performed by Treacy and Higgins [38].

The BET surface area of the synthesized adsorbent (Figure 1d) was found to be $\sim 38 \text{ m}^2/\text{g}$, while the total pore volume was $0.119 \text{ cm}^3/\text{g}$. The results obtained indicate a higher surface area when fly ash is treated with NaOH that demonstrate a good adsorption capacity for Cu^{2+} ion removal.

The chemical composition of the material, determined by EDX measurement, is listed in Table 2. The detection limit of the device was 0.08% wt.

For comparison, the results regarding the SEM and EDAX analysis for raw fly ash were included (Figure 2 and Table 3).

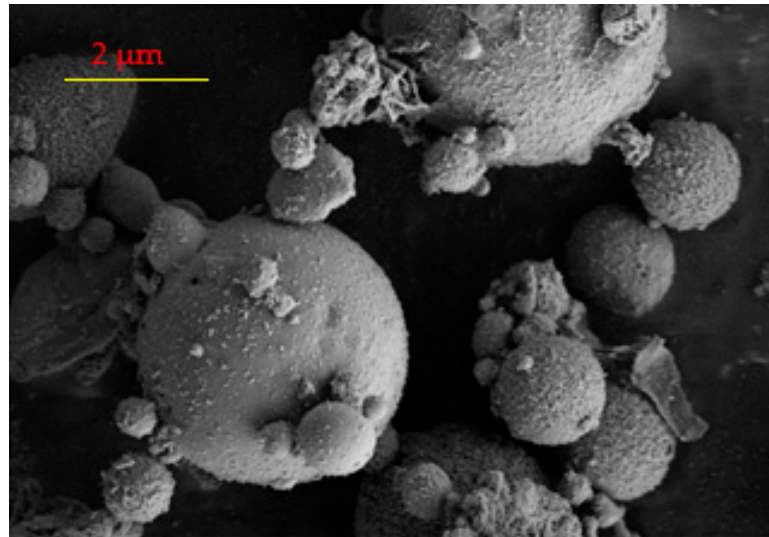


Figure 2. SEM image for raw fly ash.

Table 3. The chemical composition for raw fly ash, % atomic.

O	Na	Mg	Al	Si	K	Ca	Ti	Fe
43.32	0.79	0.62	19.19	30.81	1.75	1.15	1.54	3.05

The fly ash from CET II Holboca Iasi contains: Cu = 298 ppm, Ni = 123 ppm, Cr = 127 ppm. Other toxic metals were also presented in our previous paper [39].

The SEM image of fly ash reveals that the sample has spherical particles and small quantities of irregular shapes of the particles. On the other hand, the EDX results show differences between the composition of fly ash and synthesized material. For example, the content of Na increased from 0.79% to 3.42%.

3.2. Adsorption Experiments

The pH value is very important in the adsorption process. First of all, the influence of pH on the adsorption capacity of Cu^{2+} ion by the prepared material was investigated at pH values of 2, 3, 4 and 5 (Figure 3). The optimum pH value was found to be 5. Consequently, for further investigation regarding the influence of adsorbent dose, the initial Cu^{2+} concentration and the contact time, the pH value was kept constant at 5 in order to avoid Cu^{2+} precipitation.

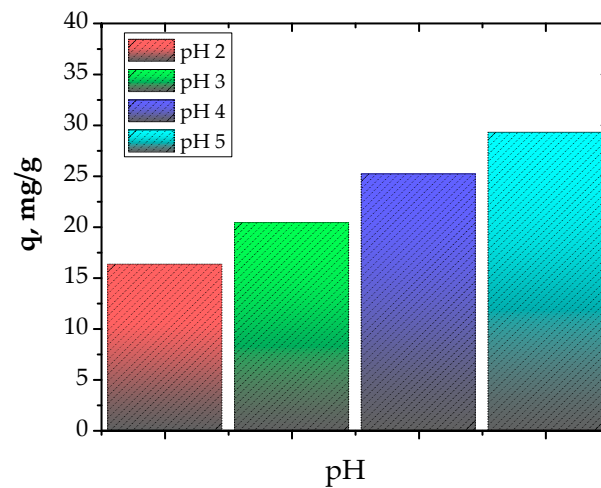


Figure 3. Influence of pH (contact time, 24 h; initial Cu^{2+} concentration, 300 mg/L; adsorbent dose, 1 g/100 mL; temperature, 25 °C).

Adsorption experiments were conducted by varying the adsorbent dose, the initial Cu^{2+} concentration and the contact time. The results regarding the influence of the adsorbent dose, the initial concentration and the contact time are presented in Figure 4.

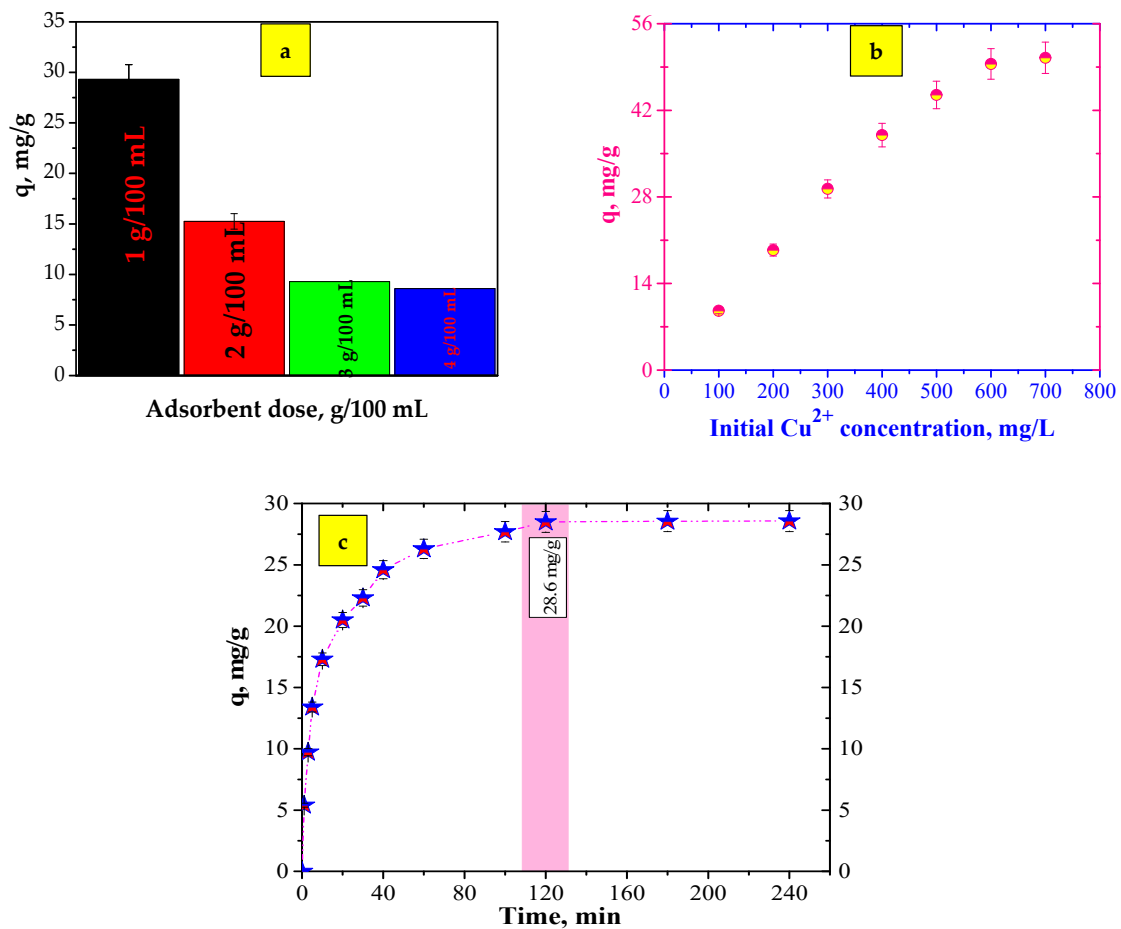


Figure 4. (a) Influence of adsorbent dose (pH, 5.0; contact time, 24 h; initial Cu^{2+} concentration, 300 mg/L; temperature, 25 °C); (b) Influence of initial concentration (pH, 5.0; contact time, 24 h; adsorbent dose, 1 g/100 mL; temperature, 25 °C); (c) Influence of contact time (pH 5.0; adsorbent dose, 1 g/100 mL; contact time, 240 min; initial Cu^{2+} concentration, 300 mg/L; temperature, 25 °C).

The influence of the adsorbent dose has a great effect on the adsorption process. The adsorbent dose influences the number of active sites available for the adsorption of pollutants [40]. The influence of the adsorbent dose on the adsorption capacity of the prepared adsorbent was investigated (Figure 4a). The effect of the adsorbent dose was performed using four dosages of the adsorbent (1–4 g/100 mL). According to Figure 4a, the adsorption capacity decreased as the adsorbent dose was increased from 1 g/100 mL to 4 g/100 mL. This fact may be attributed to the diminution of the adsorbent surface available to Cu^{2+} ions due to the agglomeration or aggregation of binding sites. The results indicated that 1 g/100 mL of synthesized material can be used for further experiments.

The initial Cu^{2+} ion concentration was studied at 100, 200, 300, 400, 500, 600 and 700 mg/L. Figure 4b presents the adsorption capacity of Cu^{2+} against the initial Cu^{2+} concentration. It is obvious that the adsorption capacity is affected by initial concentration values; thus, the adsorption capacity increased proportionally with the investigated parameter. The adsorption capacity rapidly increased when the initial concentration changed from 100 to 500 mg/L and reached the maximum adsorption capacity in the range of 600–700 mg/L. This aspect can be attributed to an increase in the driving force of Cu^{2+} ion toward the surface of synthesized material [41].

In order to study the influence of contact time on the Cu^{2+} adsorption capacity of the prepared adsorbent, the contact time was changed from 1 to 240 min. The results of the contact time are shown in Figure 4c. In the initial stage (≤ 40 min), the adsorption capacity rapidly increased due to the number of free available adsorption sites. As the contact time increased, the adsorption capacity tended to reach equilibrium. The adsorbent reached the maximum adsorption capacity of 28.6 mg/g within 120 min.

3.2.1. Adsorption Isotherms

The evaluation of adsorption isotherms was applied in order to ascertain the relationships between the prepared adsorbent and Cu^{2+} ion. The adsorption isotherm was analyzed using the Langmuir and Freundlich models [42]. All parameters corresponding to these models were calculated from the linear dependencies C_e vs. C_e/q_e and $\ln C_e$ vs. $\ln q_e$. The plots for Cu^{2+} adsorption are displayed in Figure 5.

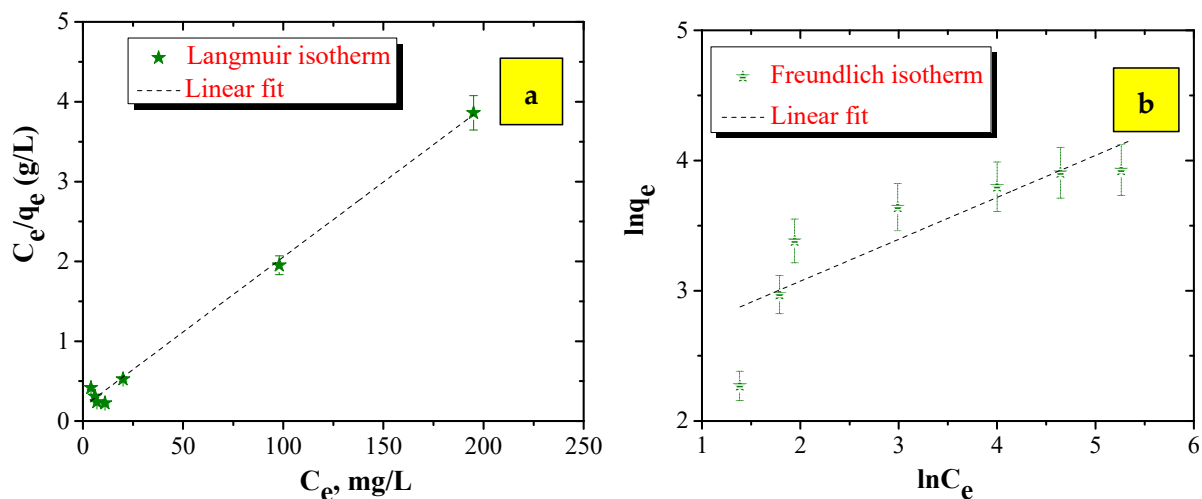


Figure 5. Langmuir (a) and Freundlich (b) isotherm plots for the adsorption of Cu^{2+} .

The values of the parameters corresponding to each isotherm model are summarized in Table 4.

Table 4. Adsorption isotherm constants.

Type of Isotherm	Equation	Linearization of Equation	Constants	R ²
Langmuir	$q_e = \frac{q_{max} \times K_L C_e}{1 + K_L C_e}$	$\frac{C_e}{q_e} = \frac{1}{K_L \times q_{max}} + \frac{C_e}{q_{max}}$	$q_{max} = 53.5 \text{ mg/g}$ $K_L = 0.094 \text{ L/g}$	0.9969
Freundlich	$q_e = K_F \times C_e^{1/n}$	$\log q_e = \left(\frac{1}{n}\right) \log C_e + \log K_F$	$K_F = 10.23 \text{ (mg/g)/(L/mg)}$ $1/n = 0.3438$	0.7413

Where: C_e (mg/L) is the concentration of metal in solution at equilibrium, q_e is the equilibrium metal adsorption capacity (mg/g), q_{max} is the maximum adsorption capacity (mg/g), K_L is the Langmuir constant (L/g), K_F is the Freundlich constant and $1/n$ is the heterogeneity factor.

The results displayed in Table 4 suggest that the adsorption of Cu^{2+} can be explained better by the Langmuir model ($R^2 \geq 0.99$), with a maximum amount of copper adsorbed of 53.5 mg/g. According to the Langmuir model, the theoretical maximum adsorption capacity and the maximum adsorption capacity of the adsorbent from the adsorption experiment were similar. The correlation coefficient of the other isotherm plot was relatively low, $R^2 = 0.7413$.

In addition, the fundamental characteristic and practicability of the Langmuir isotherm regarding a dimensionless constant separation factor or equilibrium parameter, R_L , suggest that the adsorption process of Cu^{2+} using the prepared material was favorable, Figure 6, in accord with literature [43].

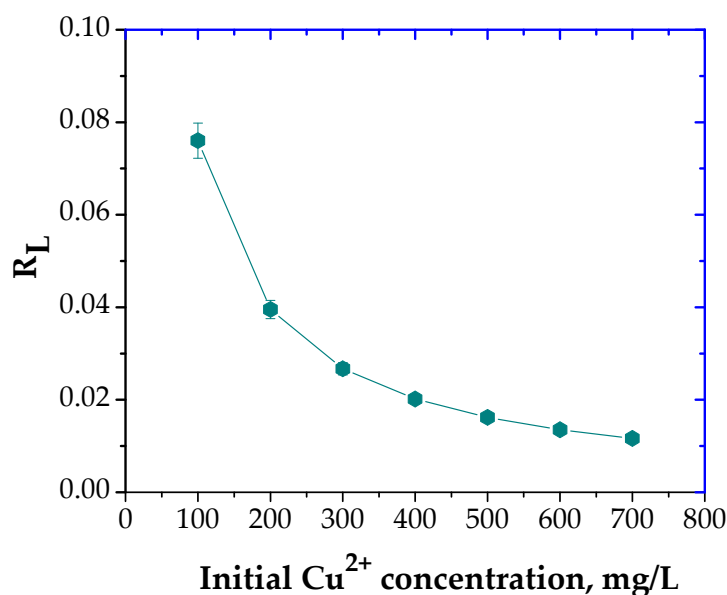


Figure 6. Plot of separation factor vs. initial Cu^{2+} initial concentration.

3.2.2. Kinetics of the Adsorption Process

Among the kinetic models developed, the pseudo-first-order and pseudo-second-order kinetic models were used to study the adsorption process of Cu^{2+} ions. The equations for the pseudo-first-order kinetic model and the pseudo-second-order kinetic model are listed in Equations (3) and (4), respectively.

$$\log(q_e - q_t) = \log q_e - \frac{(k_1 t)}{2.303} \tag{3}$$

$$\frac{t}{q_t} = \frac{1}{k_2 \times q_e^2} + \frac{t}{q_e} \tag{4}$$

where q_t is the amount of cadmium adsorbed per unit of adsorbent (mg/g) at time t , k_1 is the pseudo-first-order rate constant (1/min) and k_2 is the pseudo-second-order rate constant (g/mg min).

The slopes and intercepts of the linear plots were used in order to calculate the kinetic parameters for the adsorption of Cu^{2+} ion by prepared material. The obtained results are summarized in Table 5.

Table 5. Comparison of the kinetic models for the adsorption of Cu^{2+} .

q_e , exp (mg/g)	Pseudo-First-Order Model		Pseudo-Second-Order Model		
	k_1 , (1/min)	R^2	q_{cal} , (mg/g)	k_2 (g/mg min)	R^2
28.6	0.0419	0.9732	30	0.0028	0.9986

According to Table 5, the R^2 values obtained after fitting the data suggest that the pseudo-second-order model is more suitable than the pseudo-first-order model for describing the Cu^{2+} adsorption. The strong fit with the pseudo-second-order kinetic model suggests a chemical adsorption.

A supplementary EDX analysis after Cu^{2+} ion adsorption was performed (Figure 7). The data demonstrate that the toxic ions were attached to the surface of the prepared adsorbent.

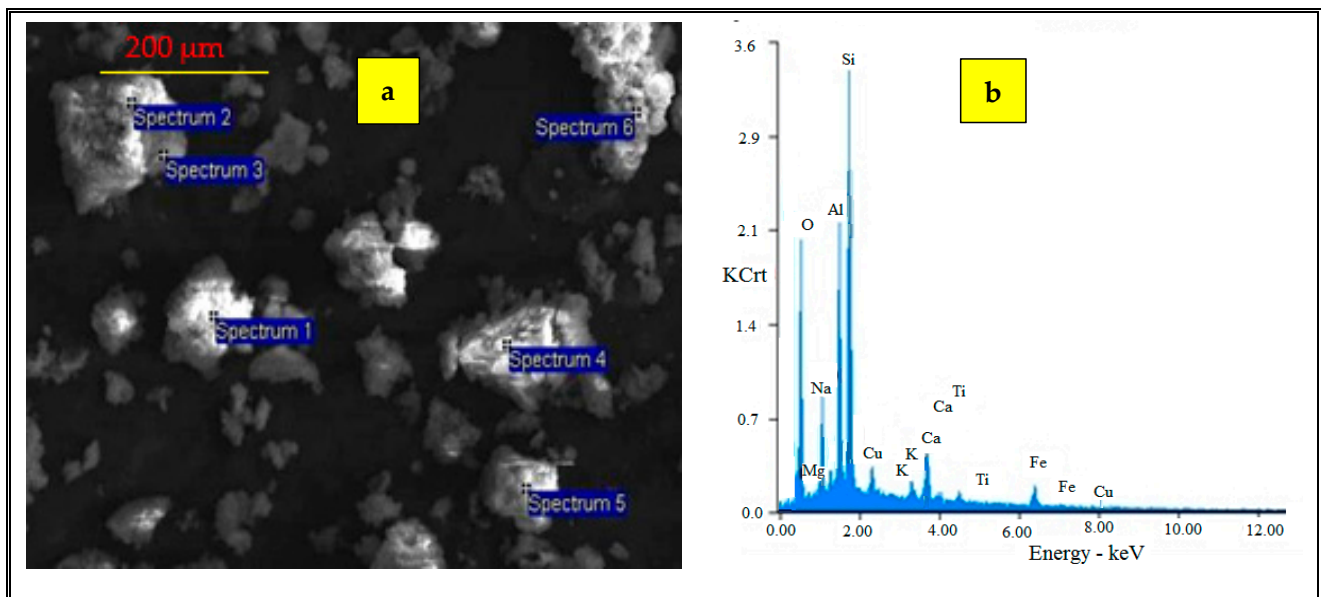


Figure 7. EDX analysis (a) after Cu^{2+} adsorption (b).

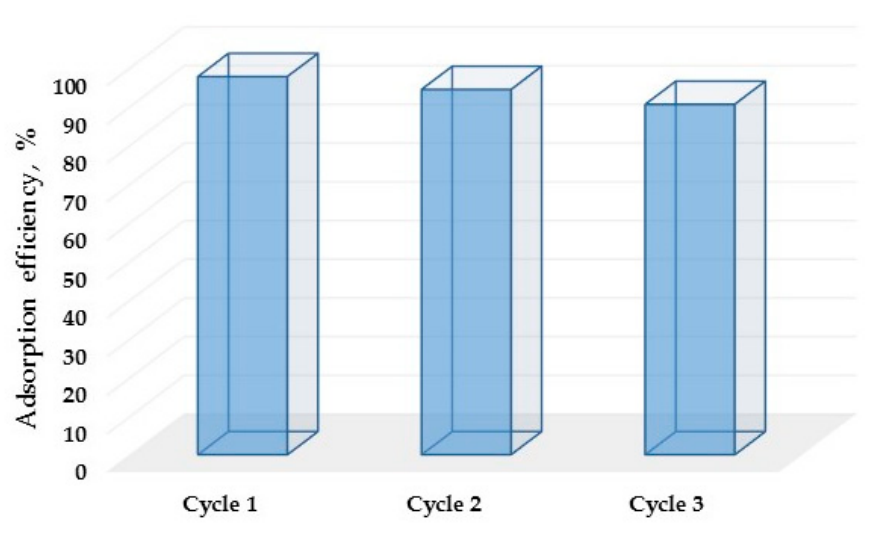
Table 6 provides a comparison of the maximum adsorption capacity (q_{max}) of treated fly ash with other previously reported studies from specialized literature.

Table 6. Comparison of adsorption capacity of various adsorbents for Cu^{2+} .

Adsorbent.	q_{max} , mg/g	Ref.
Nanosilica particles modified by Schiff base Ligands 3-methoxy salicylaldehyde propyl triethoxysilane (MNS ₁)	3.73	[44]
Nanosilica particles modified by 5-bromo salicylaldehyde propyl triethoxysilane	4.12	[44]
Nanosilica particles modified by 3-hydroxy salicylaldehyde propyl triethoxysilane (MNS ₃)	5.82	[44]
Fe_3O_4 @TETA	39.2	[45]
Fe_3O_4 @DETA	44.2	[45]
Fe_3O_4 @DAMP	52.3	[45]
Natural bentonite treated with H_2SO_4 (ARH)	17.24	[46]
Calcium homoionic clay (ARC)	18.18	[46]
Sodium homoionic clay (ARS)	24.39	[46]
Acid-treated bio-sorbent (ATB)	8	[47]
Untreated bio-sorbent (UTB)	19	[47]
Base treated bio-sorbent (BTB)	25	[47]
Detergent treated bio-sorbent (DTB)	28	[47]
Treated fly ash	53.5	This work

According to Table 6, the material prepared in this study showed good adsorption capacity.

At the end of the study, the reusability investigation of the synthesized adsorbent was performed. Experimental cycles of adsorption/desorption were performed and fed with Cu^{2+} solution during the adsorption step and 0.1 [M] HNO_3 during the desorption step. The obtained results are summarized in Figure 8.

**Figure 8.** Adsorption efficiency of the synthesized material.

From Figure 8, it is clear that the adsorption efficiency of the material drops a little after each cycle. This might be due to the amount of the adsorbent lost during the adsorption process. After three cycles the adsorption efficiency is still 90%, which made the synthesized adsorbent appropriate for use in wastewater treatment loaded with the copper ions.

4. Conclusions

The present research focused on the synthesis, characterization and applicability of one material based on the direct activation of fly ash with NaOH as an adsorbent for Cu²⁺ ion removal from aqueous media. The fly ash was synthesized under the following operating conditions: an NaOH concentration of 2M, NaOH; a fly ash ratio of 3:1; a temperature of synthesis of 90 °C; and a contact time of 6 h. In order to characterize the prepared adsorbent, SEM, EDX, XRD, FTIR and BET analyses were conducted.

The adsorption results were investigated based on two adsorption isotherms, specifically two kinetic models. The adsorption isotherms and kinetics were well described by the pseudo-second-order model and the Langmuir isotherm model. The maximum adsorption capacity for Cu²⁺ was 53.5 mg/g. The adsorption mechanism involved in the adsorption process was chemisorption.

This study demonstrated that fly ash may find application in the synthesis of low-cost adsorbents for toxic ion removal from aqueous media.

Author Contributions: M.H. and G.B.; methodology, M.H.; investigation, L.-M.T. and G.B.; resources, M.H.; writing—original draft preparation, M.H.; writing—review and editing, M.H. and G.B.; visualization, M.H.; supervision, M.H.; funding acquisition, M.H. All authors have read and agreed to the published version of the manuscript.

Funding: This work was supported by publications grant of the TUIASI, project number GI/P14/2021.

Data Availability Statement: The data presented in this study are available on request from the corresponding author.

Conflicts of Interest: The authors declare no conflict of interest.

References

1. Bhagat, S.K.; Pyrgaki, K.; Salih, S.Q.; Tiyasha, T.; Beyaztas, U.; Shahid, S.; Yaseen, Z.M. Prediction of copper ions adsorption by attapulgite adsorbent using tuned-artificial intelligence model. *Chemosphere* **2021**, *276*, 130162. [[CrossRef](#)] [[PubMed](#)]
2. Al-Saydeh, S.A.; El-Naas, M.H.; Zaidi, S.J. Copper removal from industrial wastewater: A comprehensive review. *J. Ind. Eng. Chem.* **2017**, *56*, 35–44. [[CrossRef](#)]
3. Vidu, R.; Matei, E.; Predescu, A.M.; Alhalaili, B.; Pantilimon, C.; Tarcea, C.; Predescu, C. Removal of heavy metals from wastewaters: A challenge from current treatment methods to nanotechnology applications. *Toxics* **2020**, *8*, 101. [[CrossRef](#)] [[PubMed](#)]
4. Lekgoba, T.; Ntuli, F.; Falayi, T. Application of coal fly ash for treatment of wastewater containing a binary mixture of copper and nickel. *J. Water Process. Eng.* **2021**, *40*, 101822. [[CrossRef](#)]
5. Zhao, L.X.; Liang, J.L.; Li, N.; Xiao, H.; Chen, L.Z.; Zhao, R.S. Kinetic, thermodynamic and isotherm investigations of Cu²⁺ and Zn²⁺ adsorption on Li-Al hydrotalcite-like compound. *Sci. Total Environ.* **2020**, *716*, 137120. [[CrossRef](#)]
6. Buema, G.; Lupu, N.; Chiriac, H.; Ciobanu, G.; Bucur, R.D.; Bucur, D.; Favier, L.; Harja, M. Performance assessment of five adsorbents based on fly ash for removal of cadmium ions. *J. Mol. Liq.* **2021**, *333*, 115932. [[CrossRef](#)]
7. Rukayat, O.O.; Usman, M.F.; Elizabeth, O.M.; Abosede, O.O.; Faith, I.U. Kinetic Adsorption of Heavy Metal (Copper) On Rubber (*Hevea Brasiliensis*) Leaf Powder. *S. Afr. J. Chem. Eng.* **2021**, *37*, 74–80. [[CrossRef](#)]
8. Shahrashoub, M.; Bakhtiari, S. The efficiency of activated carbon/magnetite nanoparticles composites in copper removal: Industrial waste recovery, green synthesis, characterization, and adsorption-desorption studies. *Micropor. Mesopor. Mat.* **2021**, *311*, 110692. [[CrossRef](#)]
9. Demiral, H.; Güngör, C. Adsorption of copper(II) from aqueous solutions on activated carbon prepared from grape bagasse. *J. Clean. Prod.* **2016**, *124*, 103–113. [[CrossRef](#)]
10. Katiyar, R.; Patel, A.K.; Nguyen, T.B.; Singhanian, R.R.; Chen, C.W.; Dong, C.D. Adsorption of copper (II) in aqueous solution using biochars derived from *Ascophyllum nodosum* seaweed. *Bioresour. Technol.* **2021**, *328*, 124829. [[CrossRef](#)]
11. Sudha Rani, K.; Srinivas, B.; Gourunaidu, K.; Ramesh, K.V. Removal of copper by adsorption on treated laterite. *Mater. Today Proc.* **2018**, *5*, 463–469. [[CrossRef](#)]
12. Chen, K.-Y.; Zeng, W.Y. Adsorption of Cu(II) by Poly- γ -glutamate/Apatite Nanoparticles. *Polymers* **2021**, *13*, 962. [[CrossRef](#)] [[PubMed](#)]
13. Szewczuk-Karpisz, K.; Bogatyrov, V.M.; Galaburda, M.; Sokołowska, Z. Study on Adsorption and Aggregation in the Mixed System of Polyacrylamide, Cu(II) Ions and Innovative Carbon–Silica Composite. *Polymers* **2020**, *12*, 961. [[CrossRef](#)] [[PubMed](#)]
14. Harja, M.; Buema, G.; Lupu, N.; Chiriac, H.; Herea, D.D.; Ciobanu, G. Fly Ash Coated with Magnetic Materials: Improved Adsorbent for Cu (II) Removal from Wastewater. *Materials* **2021**, *14*, 63. [[CrossRef](#)] [[PubMed](#)]

15. Lo, F.F.; Kow, K.W.; Chua, H.S.; Yeap, S.P.; Kiew, P.L.; Chan, C.H.; Yusoff, R. Magnetically aligned nanocomposite as a novel adsorbent for copper ions removal. *AIP Conf. Proc.* **2019**, *2124*, 020002. [[CrossRef](#)]
16. Munzhelele, E.P.; Ayinde, W.B.; Mudzielwana, R.; Gitari, W.M. Synthesis of Fe Doped Polyp-Phenylenediamine Composite: Co-Adsorption Application on Toxic Metal Ions (F^- and As^{3+}) and Microbial Disinfection in Aqueous Solution. *Toxics* **2021**, *9*, 74. [[CrossRef](#)]
17. Renugopal, L.; Kow, K.W.; Kiew, P.L.; Yeap, S.P.; Chua, H.S.; Chan, C.H.; Yusoff, R. Selective adsorption of copper and cadmium ions using nano-particles aligned in silica gel matrix. *AIP Conf. Proc.* **2019**, *2124*, 020001. [[CrossRef](#)]
18. Ulucan-Altuntas, K.; Uzun, H.I.; Ustundag, C.B.; Debik, E. Adsorption of copper ion from aqueous solutions by well-crystallized nanosized hydroxyapatite. *Mater. Res. Express* **2019**, *6*, 125545. [[CrossRef](#)]
19. Hamid, S.A.; Azha, S.F.; Sellaoui, L.; Bonilla-Petriciolet, A.; Ismail, S. Adsorption of copper (II) cation on polysulfone/zeolite blend sheet membrane: Synthesis, characterization, experiments and adsorption modelling. *Colloids Surf. A Physicochem. Eng. Asp.* **2020**, *601*, 124980. [[CrossRef](#)]
20. Buema, G.; Harja, M.; Lupu, N.; Chiriac, H.; Forminte, L.; Ciobanu, G.; Bucur, D.; Bucur, R.D. Adsorption Performance of Modified Fly Ash for Copper Ion Removal from Aqueous Solution. *Water* **2021**, *13*, 207. [[CrossRef](#)]
21. Park, J.H.; Eom, J.H.; Lee, S.L.; Hwang, S.W.; Kim, S.H.; Kang, S.W.; Yun, J.J.; Cho, J.S.; Lee, Y.H.; Seo, D.C. Exploration of the potential capacity of fly ash and bottom ash derived from wood pellet-based thermal power plant for heavy metal removal. *Sci. Total Environ.* **2020**, *740*, 140205. [[CrossRef](#)] [[PubMed](#)]
22. Harja, M.; Ciobanu, G. Eco-friendly Nano-adsorbents for Pollutant Removal from Wastewaters. In *Handbook of Nanomaterials and Nanocomposites for Energy and Environmental Applications*; Kharissova, O., Martínez, L., Kharisov, B., Eds.; Springer: Cham, Switzerland, 2020. [[CrossRef](#)]
23. Boycheva, S.; Zgureva, D.; Lazarova, H.; Popova, M. Comparative studies of carbon capture onto coal fly ash zeolites Na-X and Na-Ca-X. *Chemosphere* **2021**, *271*, 129505. [[CrossRef](#)] [[PubMed](#)]
24. Joseph, I.V.; Tosheva, L.; Doyle, A.M. Simultaneous removal of Cd(II), Co(II), Cu(II), Pb(II), and Zn(II) ions from aqueous solutions via adsorption on FAU-type zeolites prepared from coal fly ash. *J. Environ. Chem. Eng.* **2020**, *8*, 103895. [[CrossRef](#)]
25. Vassilev, S.V.; Vassileva, C.G. Methods for characterization of composition of fly ashes from coal-fired power stations: A critical overview. *Energy Fuels* **2005**, *19*, 1084–1098. [[CrossRef](#)]
26. Wang, C.; Yang, Z.; Song, W.; Zhong, Y.; Sun, M.; Gan, T.; Bao, B. Quantifying gel properties of industrial waste-based geopolymers and their application in Pb^{2+} and Cu^{2+} removal. *J. Clean. Prod.* **2021**, 128203. [[CrossRef](#)]
27. Predeanu, G.; Slăvescu, V.; Bălănescu, M.; Mihalache, R.D.; Marin, M.; Marin, A.C.; Drăgoescu, M.F. Coal bottom ash processing for capitalization according to circular economy concept. *Miner. Eng.* **2021**, *170*, 107055. [[CrossRef](#)]
28. Dinh, N.T.; Vo, L.N.H.; Tran, N.T.T.; Phan, T.D.; Nguyen, D.B. Enhancing the removal efficiency of methylene blue in water by fly ash via a modified adsorbent with alkaline thermal hydrolysis treatment. *RSC Adv.* **2021**, *11*, 20292–20302. [[CrossRef](#)]
29. Holler, H.; Wirsching, U. Zeolites formation from fly ash. *Fortschr. Miner.* **1985**, *63*, 21–43.
30. Sočo, E.; Kalemekiewicz, J. Removal of Copper(II) and Zinc(II) Ions From Aqueous Solution by Chemical Treatment of Coal Fly Ash. *Croat. Chem. Acta* **2015**, *88*, 267–279. [[CrossRef](#)]
31. Hałas, P.; Kołodyńska, D.; Płaza, A.; Geça, M.; Hubicki, Z. Modified fly ash and zeolites as an effective adsorbent for metal ions from aqueous solution. *Adsorp. Sci. Technol.* **2017**, *35*, 519–533. [[CrossRef](#)]
32. Darmayanti, L.; Notodarmodjo, S.; Damanhuri, E.; Mukti, R.R. Removal of Copper (II) Ions in Aqueous Solutions by Sorption onto Alkali Activated Fly Ash. *MATEC Web Conf.* **2018**, *147*, 04007. [[CrossRef](#)]
33. Paramitha, T.; Wulandari, W.; Rizkiana, J.; Sasongko, D. Performance Evaluation of Coal Fly Ash Based Zeolite A for Heavy Metal Ions Adsorption of Wastewater. *IOP Conf. Ser. Mat. Sci. Eng.* **2019**, *543*, 012095. [[CrossRef](#)]
34. Malarvizhi, T.S.; Santhi, T. Lignite fired fly ash modified by chemical treatment for adsorption of zinc from aqueous solution. *Res. Chem. Intermed.* **2013**, *39*, 2473–2494. [[CrossRef](#)]
35. Harja, M.; Buema, G.; Sutiman, D.M.; Munteanu, C.; Bucur, D. Low-cost adsorbents obtained from ash for copper removal. *Korean J. Chem. Eng.* **2012**, *29*, 1735–1744. [[CrossRef](#)]
36. Seracu, D.I. *Handbook of Analytical Chemistry*; Technic Publisher: Bucharest, Romania, 1989. (In Romanian)
37. Zare, A.; Lashanizadegan, A.; Darvishi, P.; Zerafat, M.M. Synthesis and characterization of NaP zeolite nanocrystals using [C12mim][Cl] ionic liquid. *Chem. Pap.* **2020**, *7*, 2163–2174. [[CrossRef](#)]
38. Treacy, M.M.; Higgins, J.B. *Collection of Simulated XRD Powder Patterns for Zeolites*, 5th ed.; Elsevier: Amsterdam, The Netherlands, 2007.
39. Noli, F.; Buema, G.; Misaelides, P.; Harja, M. New materials synthesized from ash under moderate conditions for removal of toxic and radioactive metals. *J. Radioanal. Nucl. Chem.* **2015**, *303*, 2303–2311. [[CrossRef](#)]
40. Tejada-Tovar, C.; Villabona-Ortiz, Á.; Gonzalez-Delgado, Á.D. Adsorption of Azo-Anionic Dyes in a Solution Using Modified Coconut (Cocos nucifera) Mesocarp: Kinetic and Equilibrium Study. *Water* **2021**, *13*, 1382. [[CrossRef](#)]
41. Eltaweil, A.S.; Injy, M.M.; Eman, M.; Abd El-Monaem, E.M.; El-Subruiti, G.M. Highly Efficient Removal for Methylene Blue and Cu^{2+} onto UiO-66 Metal–Organic Framework/Carboxylated Graphene Oxide-Incorporated Sodium Alginate Beads. *ACS Omega* **2021**, *6*, 23528–23541. [[CrossRef](#)]
42. Buema, G.; Lupu, N.; Chiriac, H.; Roman, T.; Porcescu, M.; Ciobanu, G.; Burghila, D.V.; Harja, M. Eco-Friendly Materials Obtained by Fly Ash Sulphuric Activation for Cadmium Ions Removal. *Materials* **2020**, *13*, 3584. [[CrossRef](#)]

43. Taguba, M.A.M.; Ong, D.C.; Ensano, B.M.B.; Kan, C.C.; Grisdanurak, N.; Yee, J.J.; de Luna, M.D.G. Nonlinear Isotherm and Kinetic Modeling of Cu(II) and Pb(II) Uptake from Water by MnFe₂O₄/Chitosan Nanoadsorbents. *Water* **2021**, *13*, 1662. [[CrossRef](#)]
44. Moftakhar, M.K.; Yaftian, M.R.; Ghorbanloo, M. Adsorption efficiency, thermodynamics and kinetics of Schiff base-modified nanoparticles for removal of heavy metals. *Int. J. Environ. Sci. Technol.* **2016**, *13*, 1707–1722. [[CrossRef](#)]
45. Culita, D.C.; Simonescu, C.M.; Patescu, R.E.; Preda, S.; Stanica, N.; Munteanu, C.; Oprea, O. Polyamine Functionalized Magnetite Nanoparticles as Novel Adsorbents for Cu(II) Removal from Aqueous Solutions. *J. Inorg. Organomet. Polym.* **2017**, *27*, 490–502. [[CrossRef](#)]
46. Belhadri, M.; Sassi, M.; Bengueddach, A. Preparation of Economical and Environmentally Friendly Modified Clay and Its Application for Copper Removal. *J. Water Chem. Technol.* **2019**, *41*, 357–362. [[CrossRef](#)]
47. Al Ketife, A.M.D.; Almomani, F.; Znad, H. Sustainable removal of copper from wastewater using chemically treated bio-sorbent: Characterization, mechanism and process kinetics. *Environ. Technol. Innov.* **2021**, *23*, 101555. [[CrossRef](#)]